



2024  
DISCRETE



# Penguin Decays of B mesons

Based on [JHEP 06 \(2023\) 108](#) and [JHEP 08 \(2024\) 030](#). In collaboration with Joaquim Matias, Sebastien Descotes-Genon and Gilberto Tetlalmatzi-Xolocotzi.

# Non leptonic: Motivation and Introduction

- Expectation: tensions in rare  $b \rightarrow s$  (maybe  $b \rightarrow d$  ?) if tensions in semileptonic are due to NP.
- FCNC Non leptonic decays : loop suppressed in the SM : satisfactory amount of Experimental data.
- However, increased difficulty in controlling hadronic uncertainties w.r.t semileptonic.
- Theoretical approaches available:
  - Phenomenological extraction using flavor symmetries (GTX, TH, *Eur.Phys.J.C* 82 (2022) 3, 210).
  - Relate to other modes using symmetry (U-spin, SU(3)) (MG, DL, et al., *Nucl.Phys. B* 675 (2003) 333-415 etc).
  - Compute hadronic matrix elements (QCD Factorization) (MB, MN, et al, *Phys. Lett. B* 514 (2001) 315, etc).
- Work with penguin dominated modes with  $B_{s,d}$  decaying to same final states:  $K^{(*)} \bar{K}^{(*)}, K^* \phi$ .
- Use them to construct observables (ratios of (longitudinal for vector-vector) branching ratios ). with reduced sensitivities to hadronic uncertainties (endpoint divergences).
- Use these observables to look for effects that might potentially be beyond SM: New Physics.

# Amplitude and “ $\Delta$ ”

- $\bar{A}_f = A(\bar{B}_q \rightarrow F_1 F_2) = \lambda_u^{(q)} T_q + \lambda_c^{(q)} P_q = \lambda_u^{(q)} \Delta_q - \lambda_t^{(q)} P_q$  (unitarity).

- $\Delta_q$  is free of endpoint divergences (PRL 97 (2006) 061801: SDG, JM, JV). Because:

$$T_q = A_{K^* K^*}^q \left( \alpha_4^u - \frac{1}{2} \alpha_{4,EW}^u + \beta_3^u + 2\beta_4^u - \frac{1}{2} \beta_{3,EW}^u - \beta_{4,EW}^u \right)$$

$$P_q = A_{K^* K^*}^q \left( \alpha_4^c - \frac{1}{2} \alpha_{4,EW}^c + \beta_3^c + 2\beta_4^c - \frac{1}{2} \beta_{3,EW}^c - \beta_{4,EW}^c \right)$$

- Where, Vertex Hard spectator Penguin

$$\alpha_i^p(M_1 M_2) \propto \left[ V_i(M_2) + \frac{4\pi^2}{N_c} H_i(M_1 M_2) \right] + P_i^p(M_2)$$

$$\propto X_H^{M_1} \sim \ln\left(\frac{m_b}{\Lambda_{QCD}}\right)$$

(soft gluon spectator int, divergent, power suppressed, universal)

- $\beta_i^p$ : Penguin annihilation,  $\beta_{i,EW}^p$ : Electroweak penguin annihilation

$\propto X_A^{M_1} \sim$  Endpoint divergence  $\sim \ln\left(\frac{m_b}{\Lambda_{QCD}}\right)$  (universal) **Enter the same way in T and P (at LO in QCD).**

**These divergences are responsible for the model dependence of the analysis.**

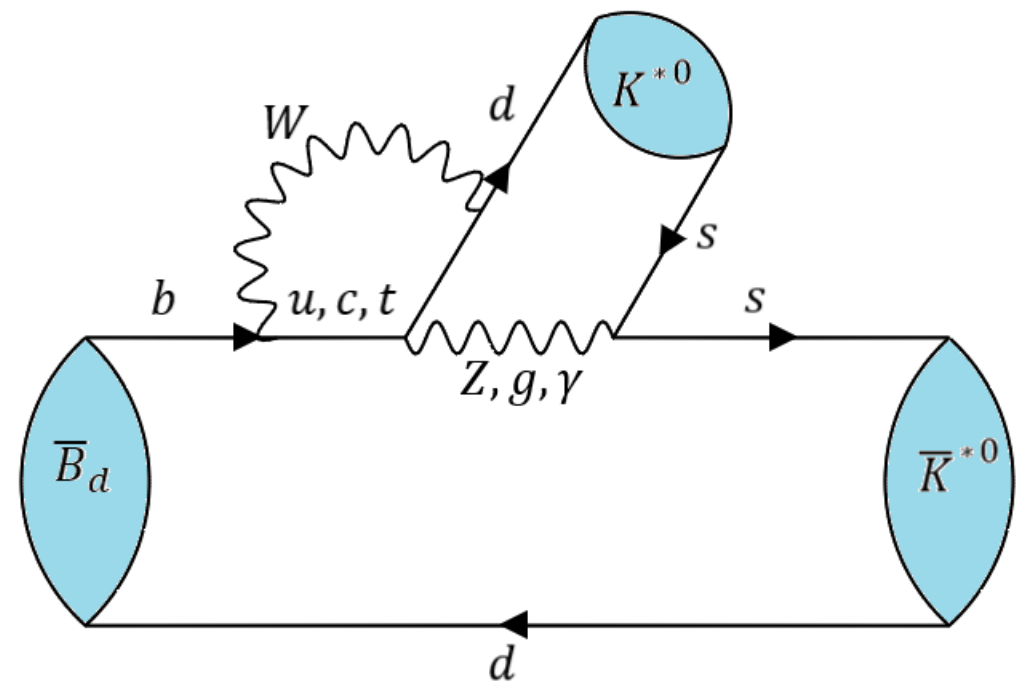
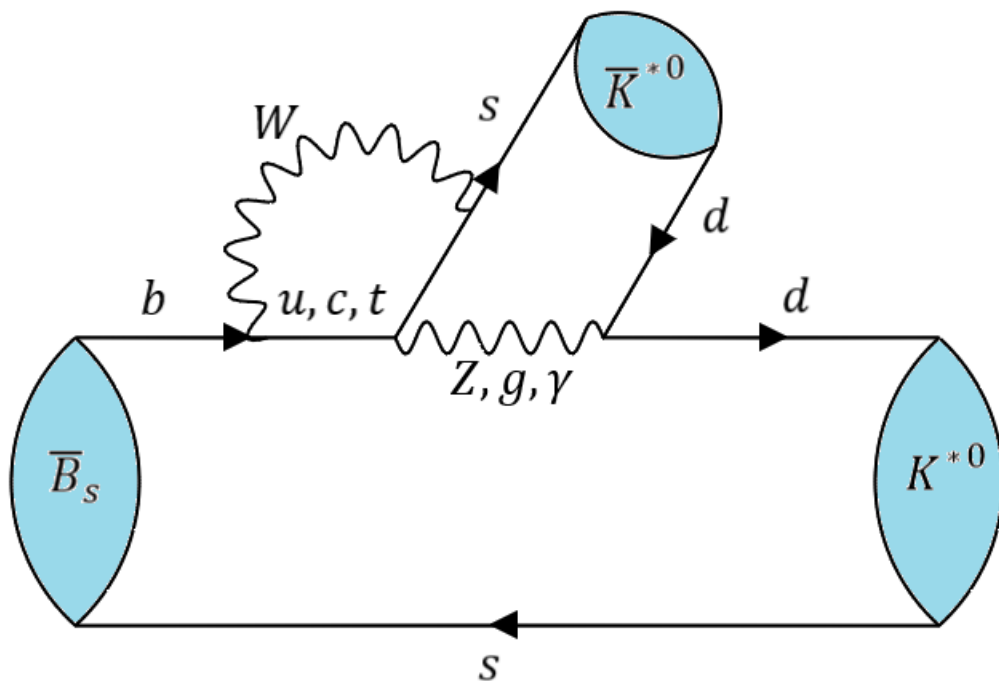
# The “L” observable: definition and features

$L = \kappa \left| \frac{P_S}{P_d} \right|^2 \frac{1 + |\alpha^S|^2 \left| \frac{\Delta_S}{P_S} \right|^2 + 2 \operatorname{Re} \left( \frac{\Delta_S}{P_S} \right) \operatorname{Re}(\alpha^S)}{1 + |\alpha^d|^2 \left| \frac{\Delta_d}{P_d} \right|^2 + 2 \operatorname{Re} \left( \frac{\Delta_d}{P_d} \right) \operatorname{Re}(\alpha^d)}$

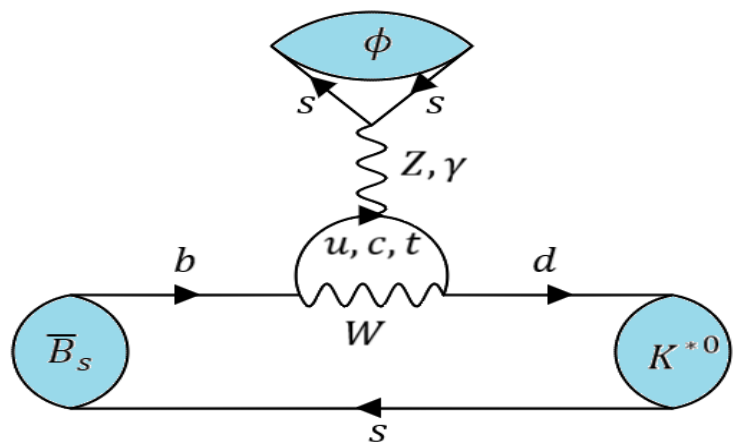
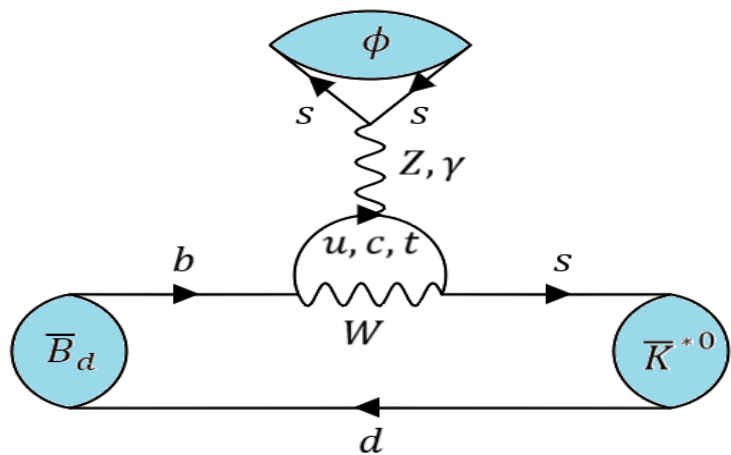
The diagram shows the definition of the observable  $L$ . It consists of a factor  $\kappa$  (circled in green) multiplied by the ratio of two terms. The numerator is  $1 + |\alpha^S|^2 \left| \frac{\Delta_S}{P_S} \right|^2 + 2 \operatorname{Re} \left( \frac{\Delta_S}{P_S} \right) \operatorname{Re}(\alpha^S)$  and the denominator is  $1 + |\alpha^d|^2 \left| \frac{\Delta_d}{P_d} \right|^2 + 2 \operatorname{Re} \left( \frac{\Delta_d}{P_d} \right) \operatorname{Re}(\alpha^d)$ . The term  $\left| \frac{P_S}{P_d} \right|^2$  is highlighted in red and labeled "Dominant contribution". The entire expression is labeled "CKM". A downward arrow from the denominator points to  $\sim 1$ .

- Relative uncertainty **less than** relative uncertainties in branching ratios.
- Generally **asymmetric** SM distribution since ratio. **Degree of asymmetry** depends on the relative uncertainty on the denominator.
- Dominant contribution** to the uncertainties from **form factors** and **not annihilation** which are dominant sources for branching ratio uncertainties (use of **u-spin symmetry**).
- Renders value of ratio ‘L’ **robust**: independent of dynamical model/symmetry considerations used to calculate its value.

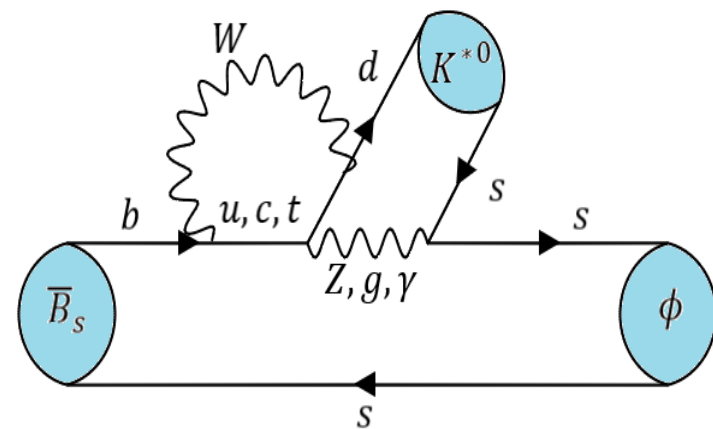
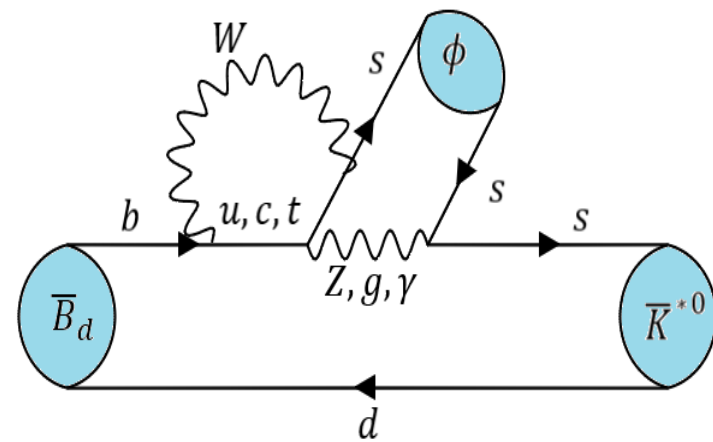
# Diagrams: $K^{(*)} \bar{K}^{(*)}$



# Diagrams: $K^{(*)}\phi$



Same as  
 $K^{(*)}K^{(*)}$



# Theory vs experiment: Current status

| Observable  | SM (QCDF)               | Experiment               | Deviation    |
|---|-------------------------|--------------------------|--------------|
| $10^6 BR(\bar{B}_d \rightarrow K^0 \bar{K}^0)$                    | $1.09^{+0.29}_{-0.20}$  | $1.21 \pm 0.16$          | $0.4\sigma$  |
| $10^7 BR(\bar{B}_d \rightarrow K^{*0} \bar{K}^{*0})_L$            | $2.27^{+0.99}_{-0.74}$  | $6.04^{+1.81}_{-1.78}$   | $1.8\sigma$  |
| $10^5 BR(\bar{B}_s \rightarrow K^0 \bar{K}^0)$                    | $2.80^{+0.89}_{-0.62}$  | $1.76 \pm 0.33$          | $1.6\sigma$  |
| $10^6 BR(\bar{B}_s \rightarrow K^{*0} \bar{K}^{*0})_L$            | $4.36^{+2.23}_{-1.65}$  | $2.62^{+0.85}_{-0.75}$   | $0.9\sigma$  |
| $10^6 BR(\bar{B}_d \rightarrow \bar{K}^{*0} \phi)_L$              | $4.53^{+2.16}_{-1.80}$  | $4.96^{+0.31}_{-0.30}$   | $0.3\sigma$  |
| $10^7 BR(\bar{B}_s \rightarrow K^{*0} \phi)_L$                    | $2.19^{+1.05}_{-0.94}$  | $5.56^{+2.78}_{-2.27}$   | $1.3\sigma$  |
| $L_{K^* \bar{K}^*}$   | $19.53^{+9.14}_{-6.64}$ | $4.43 \pm 0.92$          | $2.6\sigma$  |
| $L_{K \bar{K}}$   | $26.00^{+3.88}_{-3.59}$ | $14.58 \pm 3.37$         | $2.4\sigma$  |
| $L_{K^* \phi}$  | $22.04^{+7.06}_{-4.88}$ | $8.80^{+6.07}_{-2.97}$   | $1.5\sigma$  |
| $10^5 (BR(\bar{B}_s \rightarrow K^{*0} \bar{K}^0) + \text{c.c.})$ | $0.83^{+0.50}_{-0.25}$  | $1.98 \pm 0.28 \pm 0.50$ | $1.4\sigma$  |
| $10^6 BR(\bar{B}_d \rightarrow \bar{K}^0 \phi)$                   | $4.28^{+2.71}_{-1.50}$  | $7.3 \pm 0.7$            | $1.3\sigma$  |
| $10^6 BR(B^- \rightarrow K^- \phi)$                               | $4.67^{+2.98}_{-1.63}$  | $8.8^{+0.7}_{-0.6}$      | $1.5\sigma$  |
| $10^6 BR(B^- \rightarrow K^{*-} \phi)$                            | $4.94^{+2.34}_{-1.91}$  | $4.96^{+1.16}_{-1.08}$   | $0.05\sigma$ |

# Operator basis and SM Wilson Coefficients

$$H_{\text{eff}} = \frac{G_F}{\sqrt{2}} \sum_{p=c,u} \lambda_p^{(s,d)} \left( C_{1s,d}^p Q_{1s,d}^p + C_{2s,d}^p Q_{2s,d}^p + \sum_{i=3\dots 10} C_{is,d} Q_{is,d} + C_{7\gamma s,d} Q_{7\gamma s,d} + C_{8gs,d} Q_{8gs,d} \right)$$

$$Q_{4f} = (\bar{f}_i b_j)_{V-A} \sum_q (\bar{q}_j q_i)_{V-A}$$

$$Q_{8gf} = \frac{-g_s}{8\pi^2} m_b \bar{f} \sigma_{\mu\nu} (1 + \gamma_5) G^{\mu\nu} b$$

$$Q_{6f} = (\bar{f}_i b_j)_{V-A} \sum_q (\bar{q}_j q_i)_{V+A}$$

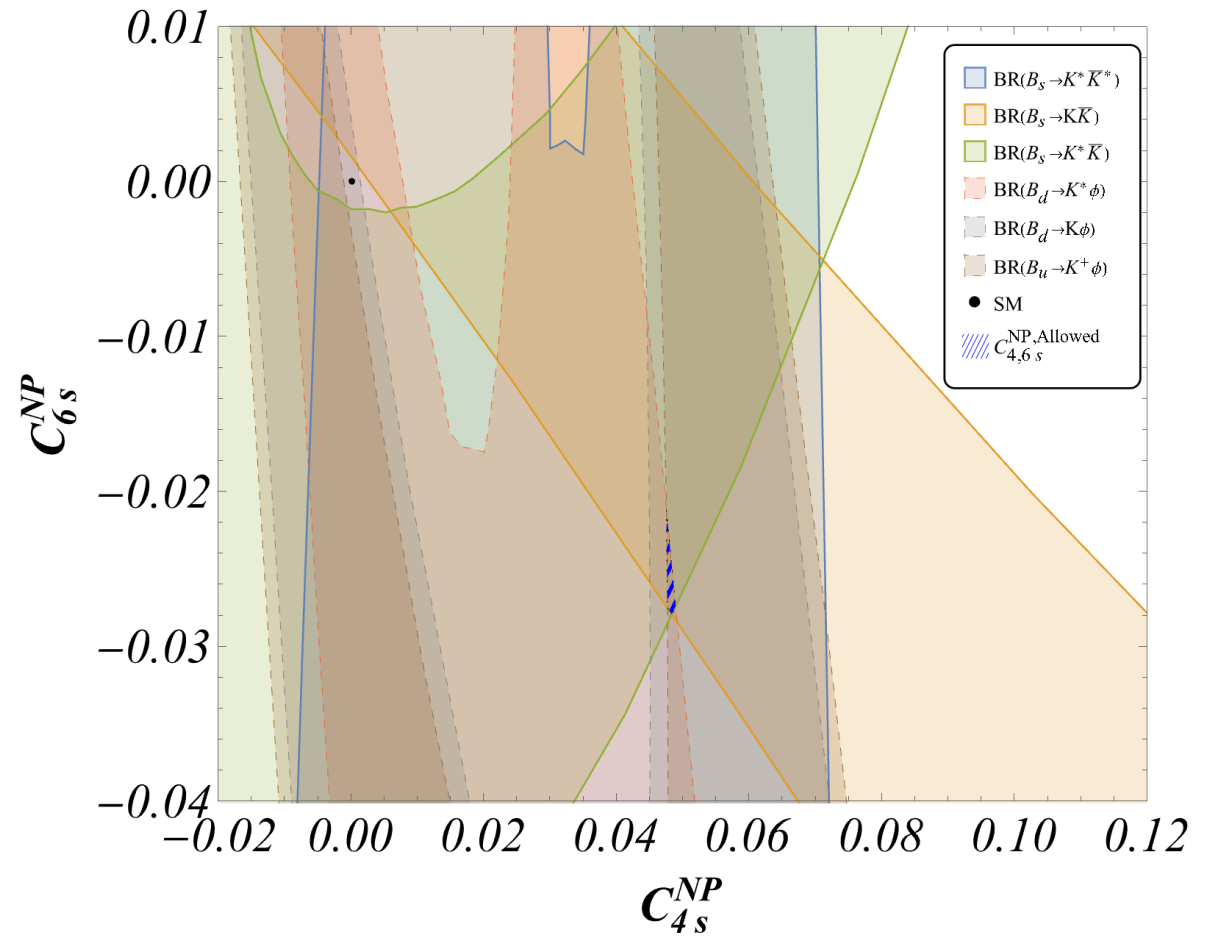
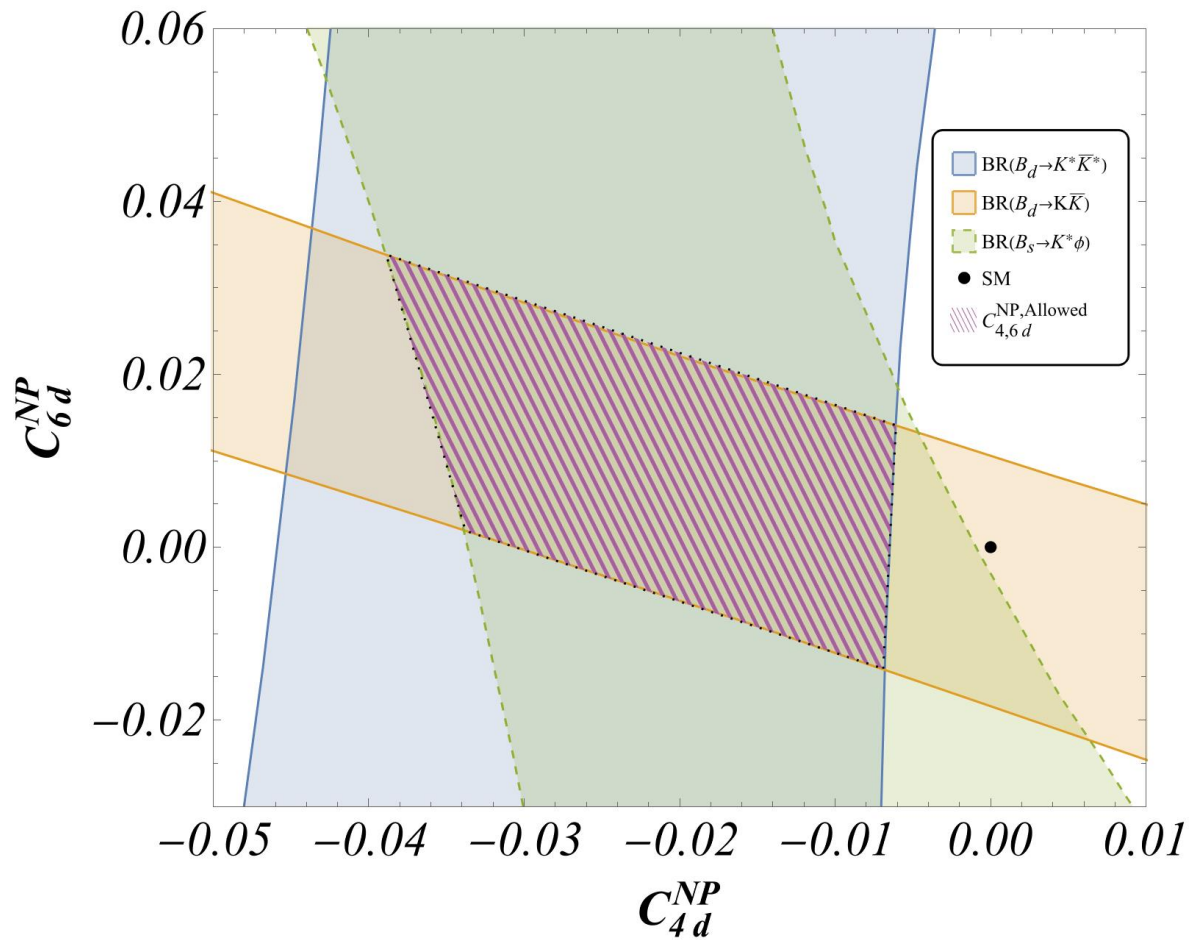
| SM Wilson Coefficients (at $\mu = 4.18 \text{ GeV}$ ) |                   |                   |                      |                            |                       |
|---|-------------------|-------------------|----------------------|----------------------------|-----------------------|
| $C_1$   | $C_2$             | $C_3$             | $C_4$                | $C_5$                      | $C_6$                 |
| 1.082   | -0.191            | 0.014             | -0.036               | 0.009                      | -0.042                |
| $C_7/\alpha_{em}$                                     | $C_8/\alpha_{em}$ | $C_9/\alpha_{em}$ | $C_{10}/\alpha_{em}$ | $C_{7\gamma}^{\text{eff}}$ | $C_{8g}^{\text{eff}}$ |
| -0.011  | 0.060             | -1.254            | 0.224                | -0.318                     | -0.151                |



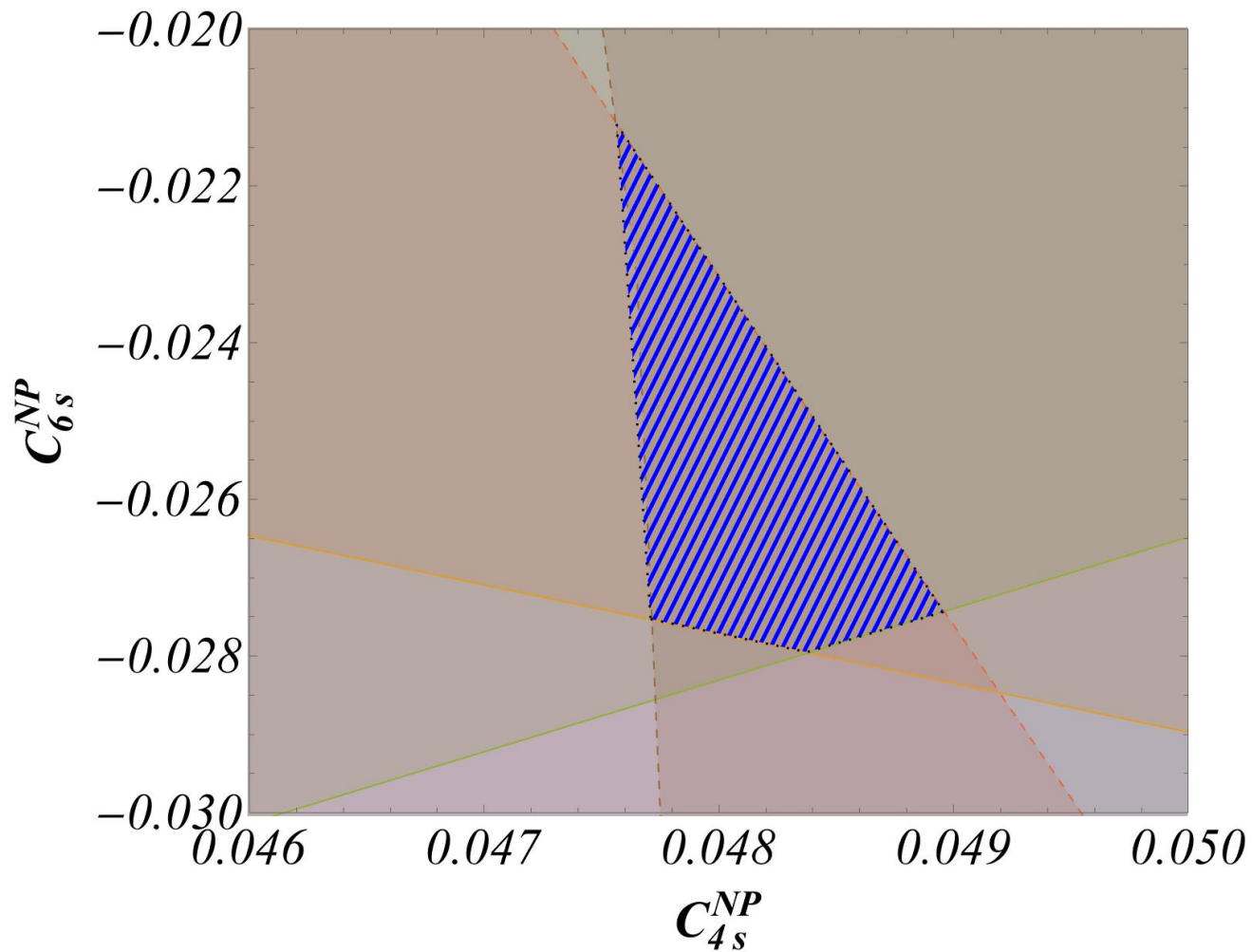
# Lessons from one operator scenarios

- NP in  $Q_{6d,s}$  does not work: because of the vector modes.
- Assuming NP affects either  $Q_{4d,s}$  or  $Q_{8gd,s}$  we find common overlaps for PP and VV modes.
- Result of including  $K^* \phi$  modes with  $K^{(*)} K^{(*)}$  modes: “allowed” range of NP values is greater for  $b \rightarrow d$  as compared to  $b \rightarrow s$ .
  - .....**pattern broken** when **pseudoscalar vector modes included**.
- NP affects  $Q_{4d,s}$ : mutual overlap among  $K^{(*)} \phi$ . Also among  $K^{(*)} K^{(*)}, K^* K$ . But not together.
- NP affects  $Q_{8gd,s}$ : mutual overlap among  $K^{(*)} \phi$ . No mutual overlap among  $K^{(*)} K^{(*)}, K^* K$ .
- No common one operator explanation is possible. **Two operators (involving  $Q_6$ )?!**
- **Appeal to Experimentalists : Updated Measurement of BR( $\bar{B}_d \rightarrow \bar{K} \phi$ ) required to confirm or dismiss this picture.**

# Two operator scenarios: $Q_4 - Q_6$

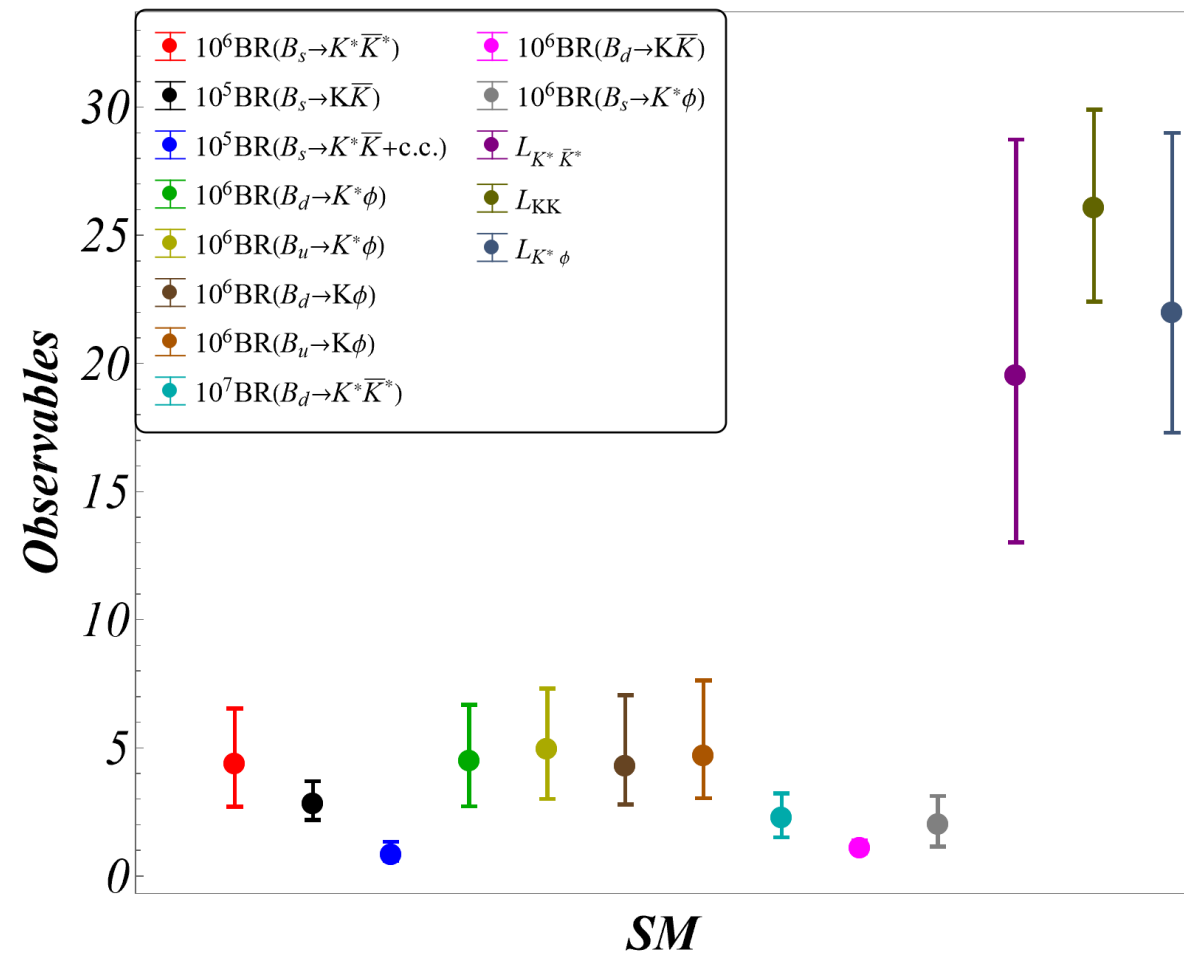
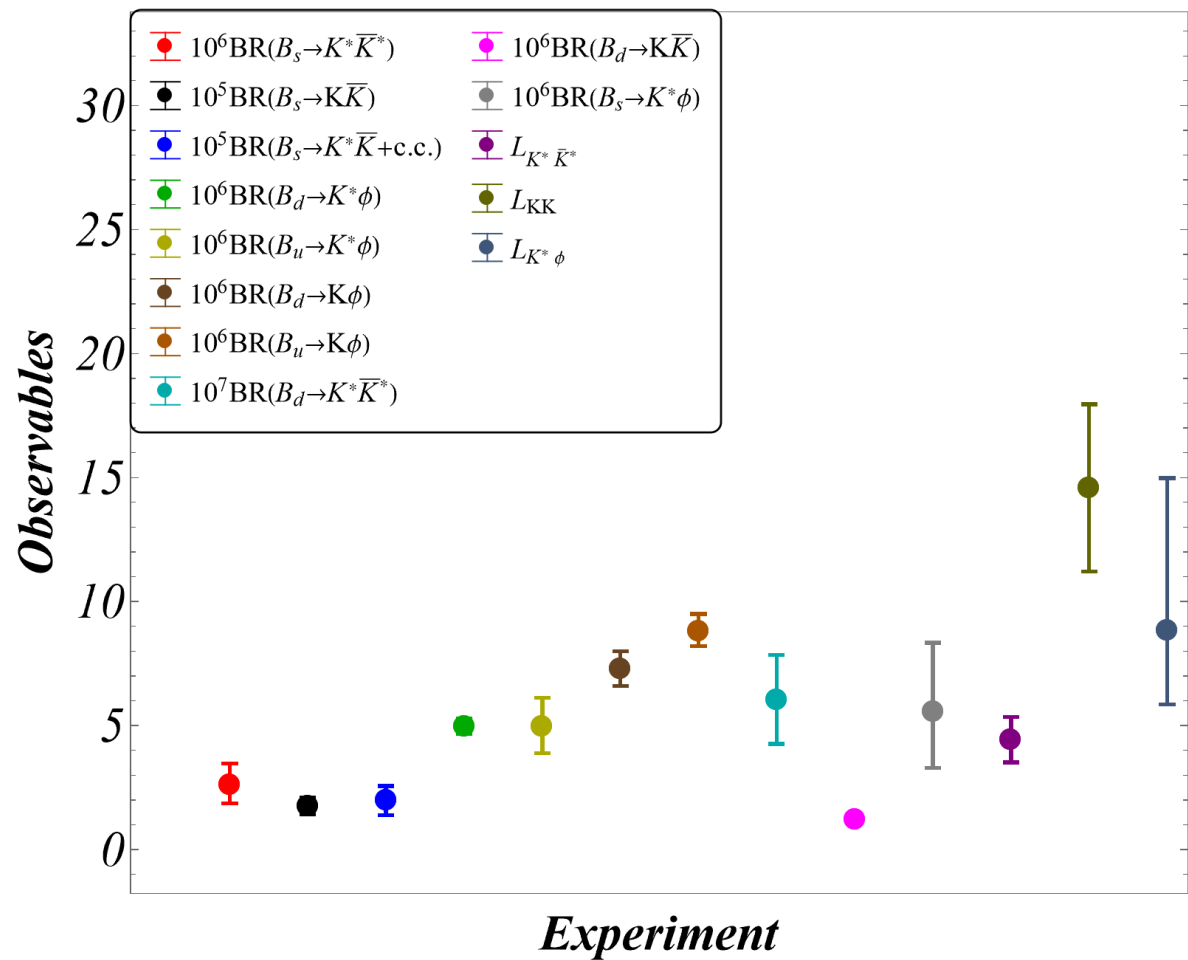


## Two operator scenarios: $Q_4 - Q_6$

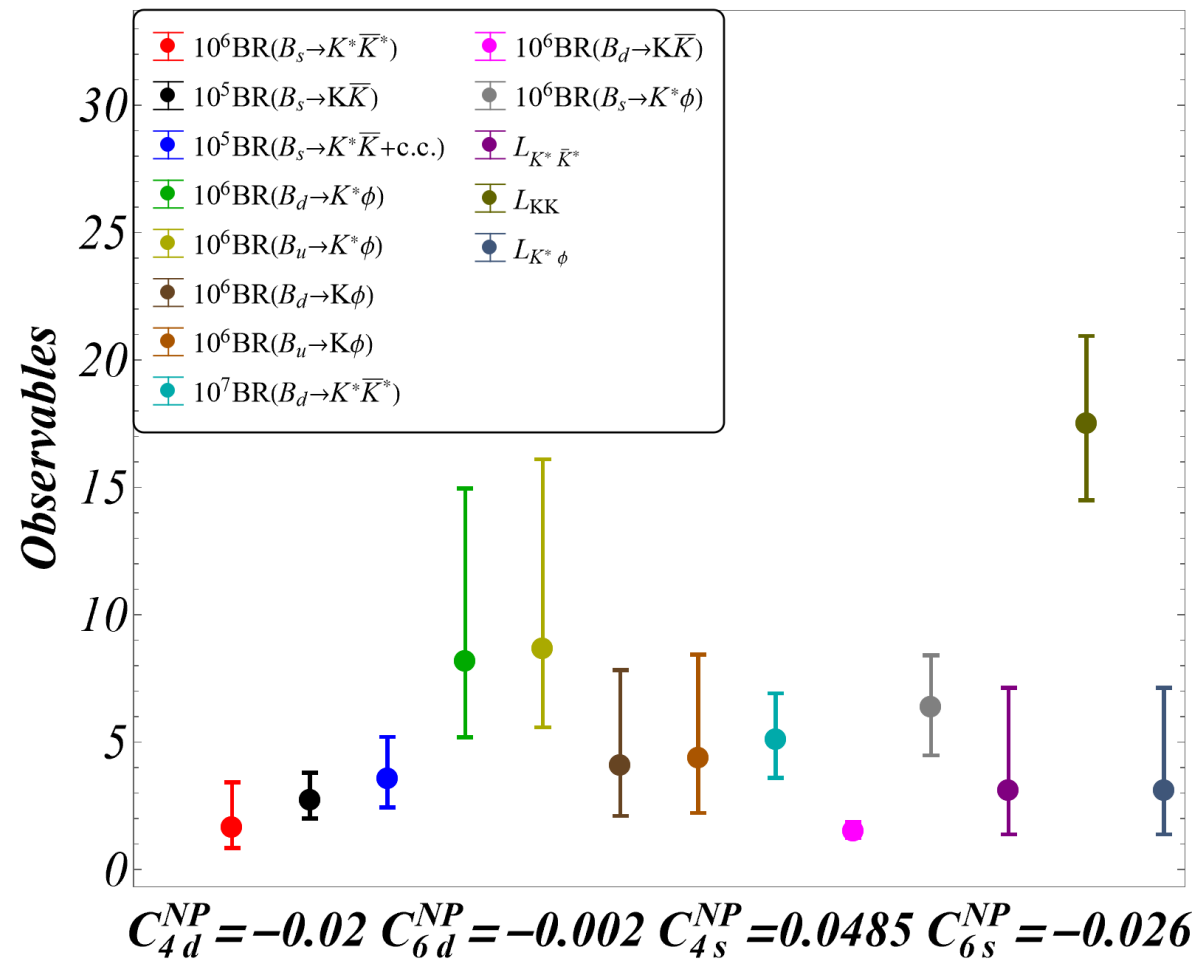
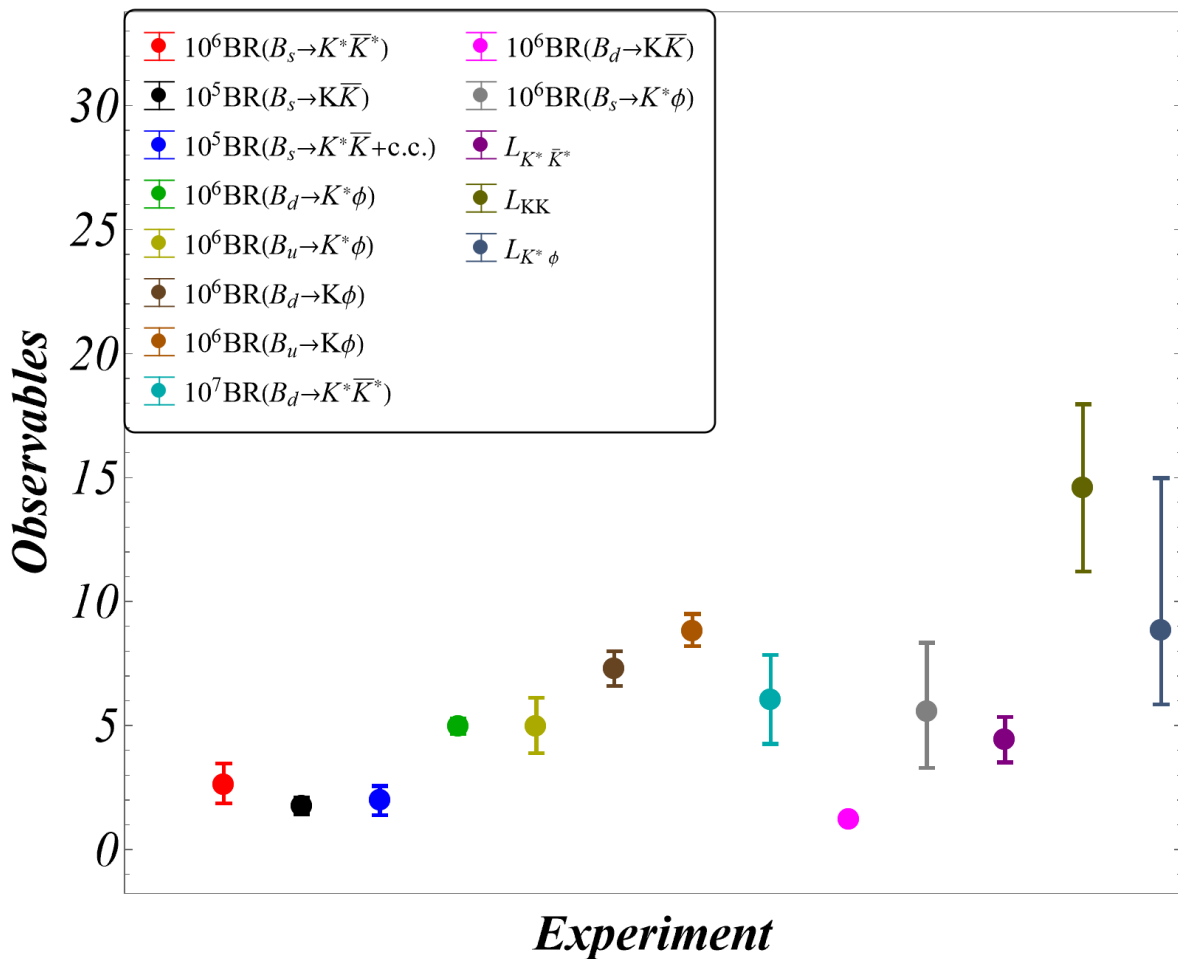


Zoomed in version showing the common region that explains **all the seven b to s branching ratios** for the  $Q_4 - Q_6$  scenario.

# Comparison: *SM*



# Comparison: $Q_4 - Q_6$



# Conclusions

- Proposed optimized “L” observables which are ratios involving penguin dominated decay modes related by d to s interchange: only used while modelling the divergent annihilation and hard spectators.

- Robust observables in terms of universal annihilation, given current (rather simplistic) model:**

| Observable         | Universal               | U spin broken            |
|--------------------|-------------------------|--------------------------|
| $L_{K^*\bar{K}^*}$ | $19.53^{+9.14}_{-6.64}$ | $19.04^{+10.20}_{-7.14}$ |
| $L_{K\bar{K}}$     | $26.00^{+3.88}_{-3.59}$ | $25.79^{+5.27}_{-4.47}$  |

- Dominant sources of uncertainties for theoretical SM estimates of the L’s are form factors .
- The simplest NP scenario that results in common overlap among all the VV, PP and PV charged and neutral branching ratios as per the current data along with the three L’s are 2 operator scenarios  $Q_{4f} - Q_{6f}$  .  **$Q_{6d,s}$  is important!**
- Appeal to Experimentalists** : Most recent measurements on  $BR(\bar{B}_d(B^-) \rightarrow \bar{K}^0(K^-)\phi)$  more than a decade old. PDG average involves measurements by CDF, Babar, CLEO, Belle with rather different central values. No LHCb measurement.  $1.5\sigma$  deviation between these measurements surprising because they are related by isospin. Maybe updated measurement can change this scenario. In particular, **these two measurements being consistent within  $1\sigma$  with the current measurement for  $BR(\bar{B}_d \rightarrow \bar{K}^0\phi)$  will make  $Q_{6f} - Q_{8gf}$  a viable scenario.**

# Future directions and discussions

- Correlated form factors (LCSR, Lattice)?
- Correlated measurement of  $K^{*0}\phi$  Branching fractions. LHCb is already working on these modes.
- **Annihilations beyond Beneke et al.** CP asymmetry measurements.
- $L_{K^*\phi}^{exp}$  has **asymmetric errors**. However, a **correlated measurement** in the future, as well as an **increase in the precision of  $f_L(\bar{B}_s \rightarrow K^{*0}\phi)$  and  $BR(\bar{B}_s \rightarrow K^{*0}\phi)$**  might help **decrease the asymmetry**. Measurement on  $b \rightarrow d$   $BR(\bar{B}_s \rightarrow K^0\phi)$  and  $BR(\bar{B}_d \rightarrow K^{*0}\bar{K}^0 + c.c.)$  will permit construction of  $L$ 's for mixed modes.
- **First exploratory works**. Working on rigorous statistical analysis taking asymmetric distributions into account. Possibility of three operator scenarios, complex Wilson coefficients etc.: Stay tuned!

THANK  
YOU!





**Backup**

# $L_{K^*K^*}$

$$L_{K^*K^*} = \kappa \left| \frac{P_s}{P_d} \right|^2 \begin{bmatrix} 1 + |\alpha^s|^2 \left| \frac{\Delta_s}{P_s} \right|^2 + 2 \operatorname{Re} \left( \frac{\Delta_s}{P_s} \right) \operatorname{Re}(\alpha_s) \\ 1 + |\alpha^d|^2 \left| \frac{\Delta_d}{P_d} \right|^2 + 2 \operatorname{Re} \left( \frac{\Delta_d}{P_d} \right) \operatorname{Re}(\alpha_d) \end{bmatrix} \rightarrow \text{CKM}$$

$1 \pm 0.3$  (Naive SU(3))

$0.91^{+0.20}_{-0.17}$  (Broken SU(3))

$0.92^{+0.20}_{-0.18}$  (QCD factorization)

**Dominant contribution**

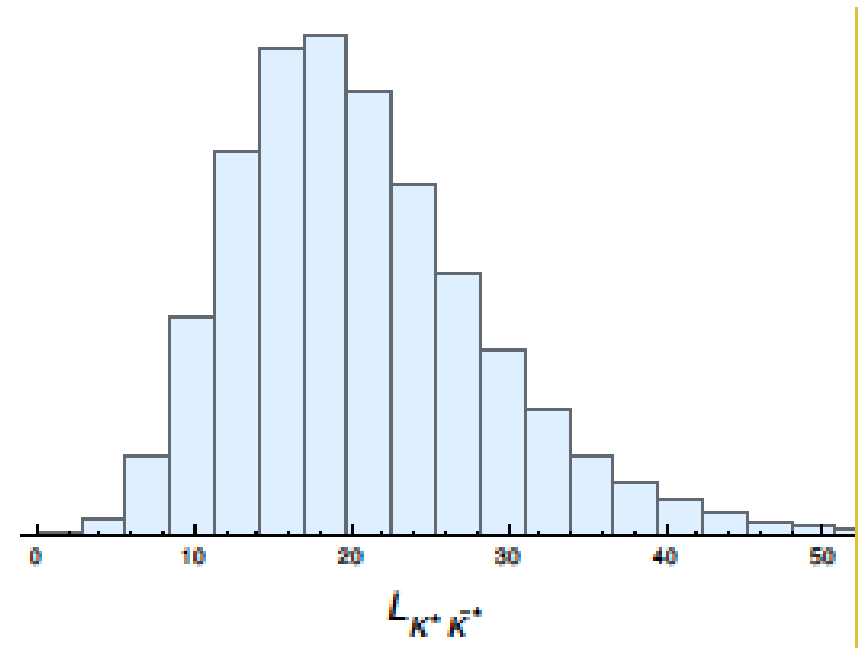
$1 \pm 0.01$

▪ **Exp:  $4.43 \pm 0.92$**

**SM:**  $23^{+16}_{-12}$  (Naive SU(3))  
 $19.2^{+9.3}_{-6.5}$  (Broken SU(3))

**$19.53^{+9.14}_{-6.64}$  (QCD factorization)**

▪ **Tension:  $2.6\sigma$**



- Note: Dominant uncertainties from form factors and NOT divergences. (Somewhat) reduced model dependence.

# $L_{K^*K^*}$ : Error Budget

| Input            | Relative Error |                |                |
|------------------|----------------|----------------|----------------|
|                  | $L_{K^*K^*}$   | $ P_s ^2$      | $ P_d ^2$      |
| $f_{K^*}$        | (-0.1%, +0.1%) | (-6.8%, +7.1%) | (-6.8%, +7%)   |
| $A_0^{B_d}$      | (-22%, +32%)   | —              | (-24%, +28%)   |
| $A_0^{B_s}$      | (-28%, +33%)   | (-28%, +33%)   | —              |
| $\lambda_{B_d}$  | (-0.6%, +0.2%) | (-4.6%, +2.1%) | (-4.1%, +1.9%) |
| $\alpha_2^{K^*}$ | (-0.1%, +0.1%) | (-3.6%, +3.7%) | (-3.6%, +3.6%) |
| $X_H$            | (-0.2%, +0.2%) | (-1.8%, +1.8%) | (-1.6%, +1.6%) |
| $X_A$            | (-4.3%, +4.4%) | (-17%, +19%)   | (-13%, +14%)   |
| $\kappa$         | (-1.4%, +2.2%) | —              | —              |
| Others           | (-1.3%, +1.1%) | (-2.7%, +2.5%) | (-1.6%, +1.6%) |

**Table 2.** Error budget of  $L_{K^*K^*}$  and  $|P_{d,s}|^2$ . The relative error of each theoretical input is obtained by varying them individually. The main sources of uncertainty are the form factors, followed by weak annihilation at a significantly smaller level.

| $B_{d,s}$ Distribution Amplitudes (at $\mu = 1$ GeV) [34, 35]                              |   |   |   |                            |                       |          |                        |
|--|---|---|---|----------------------------|-----------------------|----------|------------------------|
| $\lambda_{B_d}$ [GeV]  | $\lambda_{B_s}/\lambda_{B_d}$               |   | $\sigma_B$                                |                            |                       |          |                        |
| $0.383 \pm 0.153$  | $1.19 \pm 0.14$                             |   | $1.4 \pm 0.4$                             |                            |                       |          |                        |
| $K^*$ Distribution Amplitudes (at $\mu = 2$ GeV) [36]                                      |   |   |   |                            |                       |          |                        |
| $\alpha_1^{K^*}$   | $\alpha_{1,\perp}^{K^*}$                    | $\alpha_2^{K^*}$                              | $\alpha_{2,\perp}^{K^*}$                  |                            |                       |          |                        |
| $0.02 \pm 0.02$  | $0.03 \pm 0.03$                             | $0.08 \pm 0.06$                               | $0.08 \pm 0.06$                           |                            |                       |          |                        |
| $\phi$ Distribution Amplitudes (at $\mu = 2$ GeV) [36]                                     |   |   |   |                            |                       |          |                        |
| $\alpha_1^\phi$  | $\alpha_{1,\perp}^\phi$                     | $\alpha_2^\phi$                               | $\alpha_{2,\perp}^\phi$                   |                            |                       |          |                        |
| 0  | 0   | $0.13 \pm 0.06$                               | $0.11 \pm 0.05$                           |                            |                       |          |                        |
| Decay Constants for $B$ mesons (at $\mu = 2$ GeV) [37] and $K$ meson [28]                  |   |   |   |                            |                       |          |                        |
| $f_{B_d}$  | $f_{B_s}/f_{B_d}$                           |   | $f_K$                                     |                            |                       |          |                        |
| $0.190 \pm 0.0013$   | $1.209 \pm 0.005$                           |   | $0.1557 \pm 0.0003$                       |                            |                       |          |                        |
| Decay Constants for $K^*$ , $\phi$ , $\rho$ , $\omega$ (at $\mu = 2$ GeV) [26, 38]         |   |   |   |                            |                       |          |                        |
| $f_{K^*}$  | $f_{K^*}^\perp/f_{K^*}$                     | $f_\phi$                                      | $f_\phi^\perp/f_\phi$                     | $f_\rho$                   | $f_\omega$            |          |                        |
| $0.204 \pm 0.007$  | $0.712 \pm 0.012$                           | $0.233 \pm 0.004$                             | $0.750 \pm 0.008$                         | $0.213 \pm 0.005$          | $0.197 \pm 0.008$     |          |                        |
| $B_{d,s} \rightarrow K^*$ , $\phi$ form factors [26] and B-meson lifetimes (ps) [39]       |   |   |   |                            |                       |          |                        |
| $A_0^{B_s \rightarrow K^*}(q^2 = m_\phi^2)$  | $A_0^{B_d \rightarrow K^*}(q^2 = m_\phi^2)$ | $A_0^{B_s \rightarrow \phi}(q^2 = m_{K^*}^2)$ | $\tau_{B_d}$                              | $\tau_{B_s}$               |                       |          |                        |
| $0.380 \pm 0.024$  | $0.393 \pm 0.039$                           | $0.438 \pm 0.024$                             | $1.519 \pm 0.004$                         | $1.520 \pm 0.005$          |                       |          |                        |
| Mass and decay widths for $\rho$ , $\omega$ (GeV) [28]                                     |   |   |   |                            |                       |          |                        |
| $m_\rho$   | $\Gamma_\rho$                               | $m_\omega$                                    | $\Gamma_\omega$                           |                            |                       |          |                        |
| 0.7745   | 0.1484                                      | 0.7827  | 0.0087                                    |                            |                       |          |                        |
| $B_d \rightarrow K$ [25], $B_s \rightarrow K$ [40] and $B_s \rightarrow \phi$ form factors |   |   |   |                            |                       |          |                        |
| $f_0^{B_s}(q^2 = m_\phi^2)$  | $f_0^{B_d}(q^2 = m_\phi^2)$                 |   | $A_0^{B_s \rightarrow \phi}(q^2 = m_K^2)$ |                            |                       |          |                        |
| $0.336 \pm 0.023$  | $0.340 \pm 0.011$                           |   | $0.426 \pm 0.024$                         |                            |                       |          |                        |
| Wolfenstein parameters [41]  |   |   |   |                            |                       |          |                        |
| $A$  | $\lambda$                                   | $\bar{\rho}$                                  | $\bar{\eta}$                              |                            |                       |          |                        |
| $0.8132^{+0.0119}_{-0.0060}$   | $0.22500^{+0.00024}_{-0.00022}$             | $0.1566^{+0.0085}_{-0.0048}$                  | $0.3475^{+0.0118}_{-0.0054}$              |                            |                       |          |                        |
| QCD scale and masses [GeV] [28]  |   |   |   |                            |                       |          |                        |
| $\bar{m}_b(\bar{m}_b)$   | $m_b/m_c$                                   | $m_{B_d}$                                     | $m_{B_s}$                                 | $m_{K^*}$                  | $m_\phi$              | $m_K$    | $\Lambda_{\text{QCD}}$ |
| 4.18   | $4.577 \pm 0.008$                           | 5.27966                                       | 5.36692                                   | 0.89555                    | 1.01946               | 0.497611 | 0.225                  |
| SM Wilson Coefficients (at $\mu = 4.18$ GeV)   |   |   |   |                            |                       |          |                        |
| $C_1$  | $C_2$                                       | $C_3$   | $C_4$                                     | $C_5$                      | $C_6$                 |          |                        |
| 1.082  | -0.191                                      | 0.014   | -0.036                                    | 0.009                      | -0.042                |          |                        |
| $C_7/\alpha_{em}$  | $C_8/\alpha_{em}$                           | $C_9/\alpha_{em}$                             | $C_{10}/\alpha_{em}$                      | $C_{7\gamma}^{\text{eff}}$ | $C_{8g}^{\text{eff}}$ |          |                        |
| -0.011   | 0.060                                       | -1.254  | 0.224                                     | -0.318                     | -0.151                |          |                        |

|  | <i>MLR</i>             | <i>CDF</i>             |
|--|------------------------|------------------------|
| $L_{K \cdot \bar{K} \cdot}$                                    | $17.2^{+8.3}_{-5.9}$   | $19.5^{+9.1}_{-6.7}$   |
| $L_{K\bar{K}}$   | $25.5^{+4.0}_{-3.3}$   | $26.0^{+3.9}_{-3.6}$   |
| $\hat{L}_{K \cdot}$  | $20.5^{+6.8}_{-6.2}$   | $21.3^{+7.2}_{-6.3}$   |
| $\hat{L}_K$  | $25.3^{+3.7}_{-4.5}$   | $25.0^{+4.2}_{-4.1}$   |
| $L_{K \cdot}$  | $16.6^{+6.9}_{-6.0}$   | $17.4^{+6.6}_{-5.8}$   |
| $L_K$  | $28.8^{+5.2}_{-4.6}$   | $29.2^{+5.5}_{-5.3}$   |
| $L_{\text{total}}$   | $23.5^{+3.8}_{-4.0}$   | $23.5^{+4.0}_{-3.8}$   |
| $R_d$  | $0.67^{+0.23}_{-0.24}$ | $0.70^{+0.30}_{-0.22}$ |
| $\mathcal{B}(B_d \rightarrow K^{*0} \bar{K}^{*0}) \times 10^6$ | $0.22^{+0.08}_{-0.08}$ | $0.23^{+0.10}_{-0.08}$ |
| $\mathcal{B}(B_s \rightarrow K^{*0} \bar{K}^{*0}) \times 10^6$ | $3.95^{+1.88}_{-1.54}$ | $4.36^{+2.23}_{-1.65}$ |
| $\mathcal{B}(B_d \rightarrow K^0 \bar{K}^0) \times 10^6$       | $1.01^{+0.24}_{-0.16}$ | $1.09^{+0.29}_{-0.20}$ |
| $\mathcal{B}(B_s \rightarrow K^0 \bar{K}^0) \times 10^6$       | $25.6^{+7.5}_{-5.2}$   | $28.0^{+8.9}_{-6.2}$   |

$\alpha_j$  coefficients  $\rightarrow a_j$  [BBNS]

$$a_i^p(M_1 M_2) = \left( C_i + \frac{C_{i\pm 1}}{N_c} \right) N_i(M_2) + \frac{C_{i\pm 1}}{N_c} \frac{C_F \alpha_s}{4\pi} \left[ V_i(M_2) + \frac{4\pi^2}{N_c} H_i(M_1 M_2) \right] + P_i^p(M_2),$$

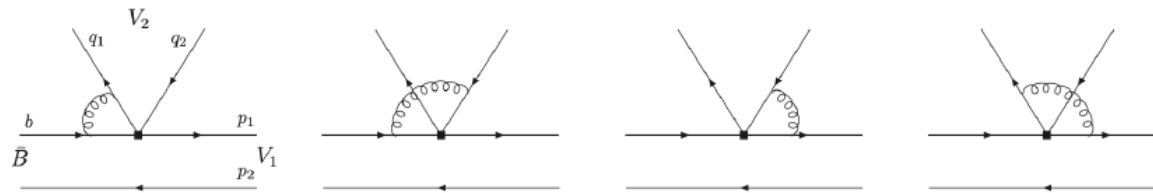


Figure 1: Vertex diagrams.

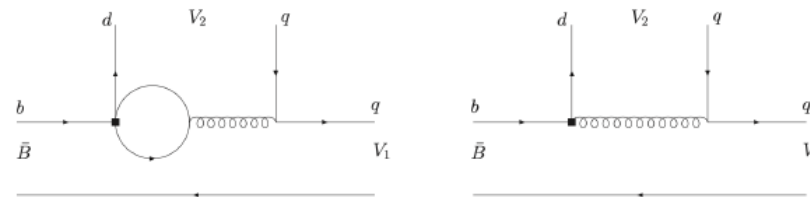


Figure 2: Penguin diagrams.

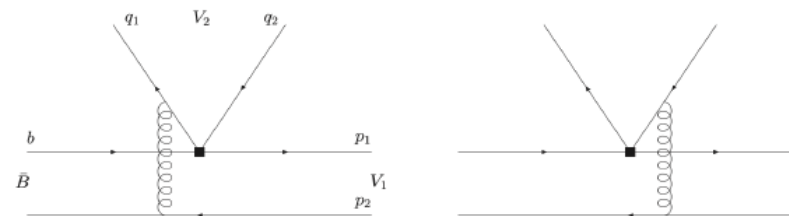


Figure 3: Hard spectator diagrams.

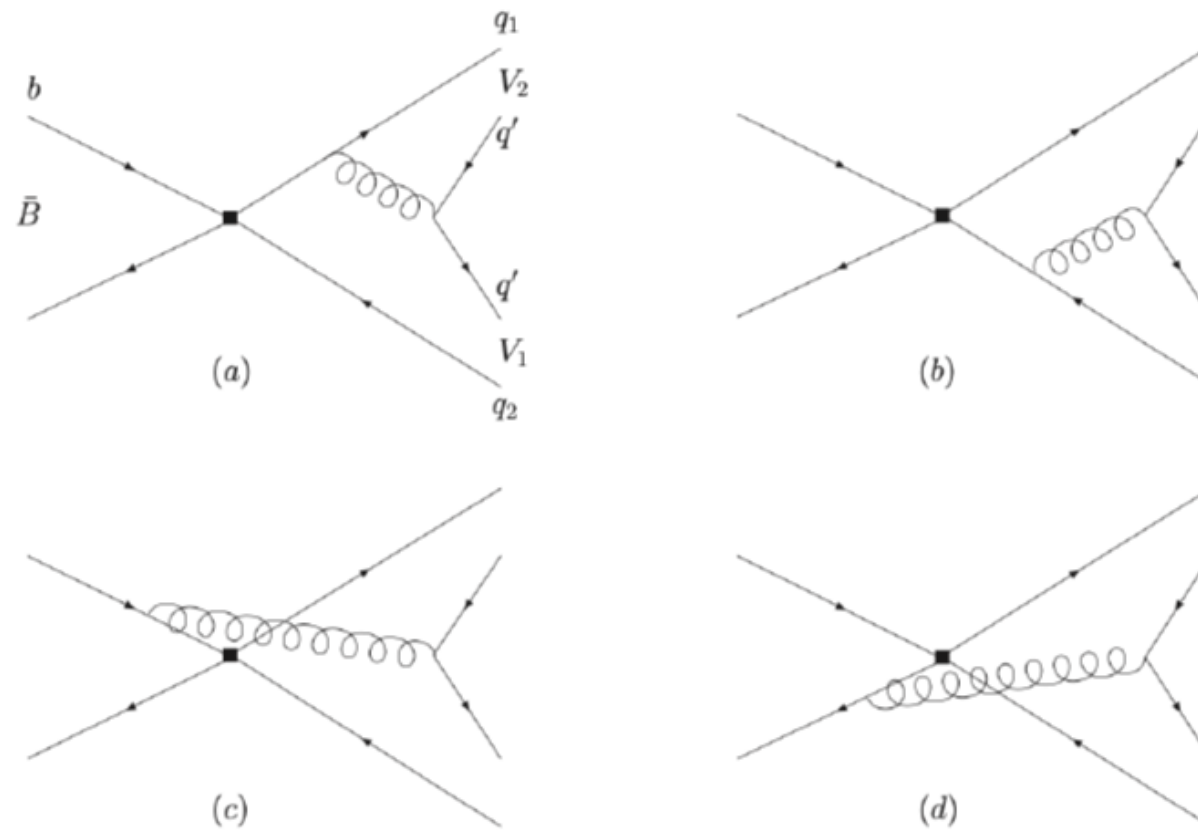


Figure 4: Annihilation diagrams.

**Main caveat:**

(Existence of some) **Power suppressed** but **IR divergent** spectator scattering and weak annihilation that affects amplitudes:

